Journal of Sound and Vibration (2000) **233**(2), 329–352
doi:10.1006/jsvi.1999.2799, available online at http://www.idealibrary.com on IDEAL®

USE OF A TORSIONAL WAVE SENSOR TO MEASURE THE LEVEL OF A COMPRESSIBLE FLUID

A. GOUBEL-LENOËL

CEA Cadarache - DER/SSAE/LSMR 13108 *St-Paul-lez-Durance cedex, France*

P. J. T. FILIPPI

Laboratoire de Mécanique et d'Acoustique, 31 *chemin Joseph Aiguier*, 13402 *Marseille cedex* 20, *France*

AND

C. LHUILLIER

CEA Cadarache - DER/SSAE/LSMR 13108 *St-Paul-lez-Durance cedex, France*

(*Received* 30 *June* 1999, *and in final form* 23 *November* 1999)

In nuclear pressurized water reactors, information about fluid masses or fluid levels is required, especially in the reactor vessel, where the core of the reactor must be immersed, to avoid damage or accidents. To reinforce the existing instrumentation, the possibilities of an immersed torsional wave sensor (that is, an elastic solid waveguide) have already been looked into and modelled, considering an incompressible surrounding fluid. Yet, in case of depressurization, the fluid can turn into a two-phase fluid. This is the reason why a way to extend the existing model has been investigated. As a first step, in this paper, the compressibility of the surrounding fluid has been taken into account.

Some assumptions have been made: the transverse dimensions of the waveguide are small compared to its length and the wavelengths in the fluid. The focus is on a cylindrical waveguide, with an elliptic cross-section. Use is made of elliptic co-ordinates and Mathieu functions. The analysis starts with the elasticity equations for the waveguide. Then, from the exact expression of the pressure exerted by the fluid on the waveguide boundary, a long-wavelength approximation is obtained. In the end, the principle of energy conservation is applied, leading to an approximate equation governing the fluid-loaded waveguide motion. Finally, some simulations are made, highlighting the influence of the compressibility.

1. INTRODUCTION

1.1. SHORT DESCRIPTION OF A NUCLEAR PRESSURIZED WATER REACTOR

To make the context of the work clear, a summary of the principle of a nuclear pressurized water reactor (PWR) is given. A nuclear power station aims at generating vapor at high pressure, the expansion of which makes a turbine turn, driving the alternating-current generator. The PWR is a reactor with separated circuits of thermic transfer (see Figure 1).

- The *primary* circuit, a closed cooling circuit, ensures heat transfer from the core to the secondary circuit. In this circuit, the pressurized water flows through the core, where nuclear reactions take place, and picks up heat from it.

0022-460X/00/220329 + 24 $35.00/0

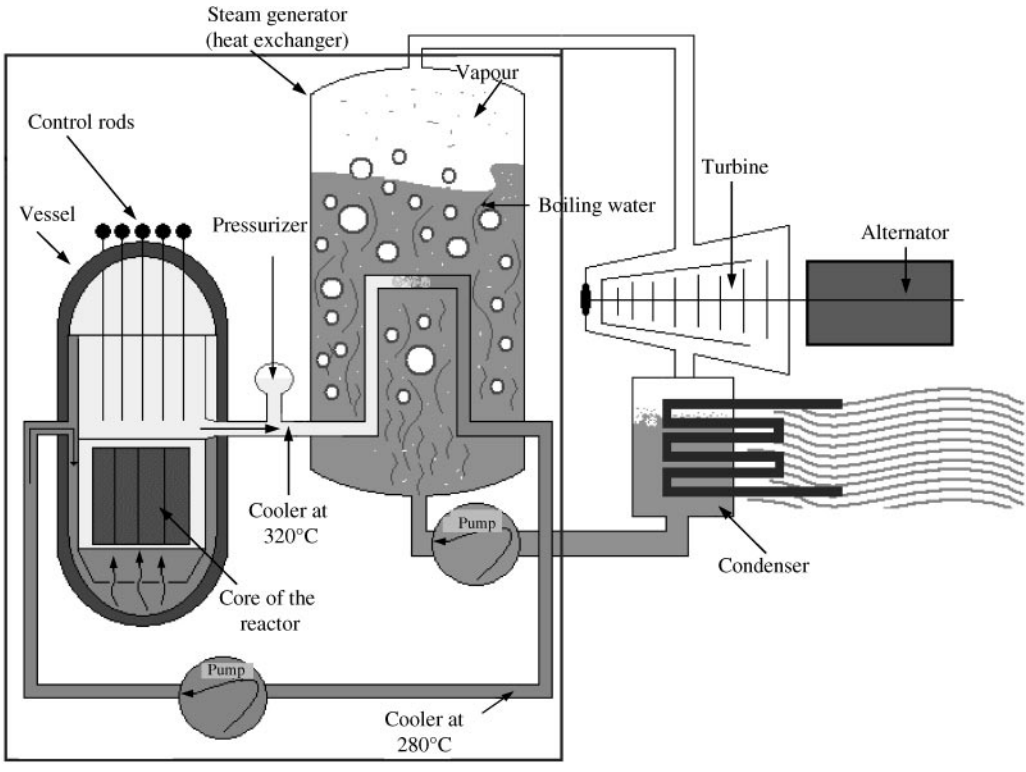

Figure 1. Scheme of a pressurized water reactor (from a document from the French Atomic Energy Commission).

- This primary circuit water is then able to heat the *secondary* circuit water up to boiling temperature. Steam is produced, which works the turbine.

For the steam to have the required characteristics (of temperature and pressure), the primary fluid needs to have a temperature as high as possible (about 300°C), which implies a high pressure too (about $1{\cdot}55 \times 10^7$ Pa).

Now focus on the reactor vessel, which is 13 m high and has a diameter of 4 m. It contains the core and the primary water. The core, where the nuclear reactions take place, consists of fuel assemblies forming a cylinder. The primary water

- takes heat from the core and transfers it to the steam generator;
- acts as a moderator, to partly control the reactivity of the nuclear reactor (it contains boron, which absorbs neutrons).

This is the reason why water level measurement is such an important matter. There must be enough water, to avoid both core damage and nuclear accidents.

1.2. THE TORSIONAL WAVE SENSOR

The need for water level control has been highlighted. Now a way to measure the water level, or *equivalent* water level is sought. Indeed, in case of depressurization in the primary

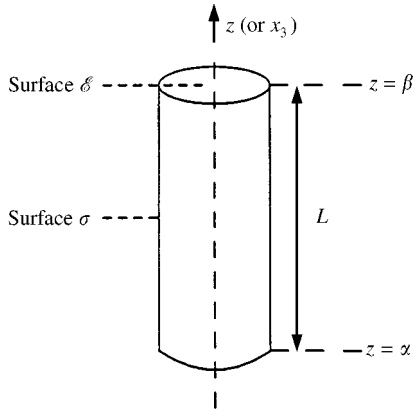

Figure 2. Some geometric definitions for the torsional wave sensor.

circuit, the fluid can turn into a two-phase fluid (water with steam bubbles), and engineers are interested in knowing the level which would be effective after repressurization.

At the present time, in pressurized water reactor vessels, the water level is controlled by means of a differential pressure sensor, which measures the difference of pressure between the top and the bottom of the vessel. The level is then derived. For future reactors, alternative methods are sought, which would avoid going through the bottom of the vessel. Most of the traditional methods aiming at measuring levels use technologies which are not compatible with the physical environment of reactor vessels (for example, the design of the vessel and of its internal structures strongly limits the possibilities of non-invasive ultrasonic techniques). Among the possible solutions, the French Atomic Energy commission is investigating the possibilities of the torsional wave sensor, which would allow a continuous monitoring.

Now focus on the means of measuring the water level. A torsional wave of finite duration is propagated in a waveguide of a non-circular cross-section. It is generated at one end of the waveguide and reflected at the other end. The reflected wave is then detected by the same transducer which has generated it. The propagation time is measured, and information about the fluid surrounding the waveguide (density, level, etc.) can then be inferred, using the theoretical model.

The following notation is used (see Figure 2). Consider a cylinder of length L and axis z, with $\alpha \leqslant z \leqslant \beta$. The surface of its cross-section is denoted by $\mathscr{E}$, and its lateral surface is called σ.

1.3. PREVIOUS WORKS

To begin with, Lynnworth, from the Panametrics company, experimentally showed a relation between the phase velocity of a torsional wave propagating in a waveguide of a non-circular cross-section and the liquid density of the surrounding fluid. In 1979, Arave [1] related experiments carried out in two-phase fluids.

The theoretical aspect was then tackled by Bau [2] in 1986, for an *incompressible* surrounding fluid. In 1987, Wang's [3] works took the *viscosity* of the fluid into account. In 1989, Kim [4] looked for the best geometry of the waveguide. In 1993, some applications for two-phase fluids, with separated phases, were published [5].

Afterwards, these authors stopped working on that subject. Some improvements were proposed by other authors (for example, taking the effects of the temperature into account [6]), but still considering an *incompressible* surrounding fluid.

Yet, in a reactor vessel, the fluid can turn into a two-phase fluid, which leads one to consider the presence of bubbles. As a first step, a model which allows the fluid to be compressible is developed in this paper. Its viscosity is not taken into account, but can easily be introduced when a two-phase fluid is considered (for example, a complex density ρ_f and a complex sound velocity c_f in the fluid can be accounted for). Part of the work is to look for an expression of the apparent phase velocity of the torsional wave which would take the compressibility of the surrounding fluid into account. It will be compared to that given in the above-mentioned articles, for an incompressible fluid:

$$c = \sqrt{\frac{\mu J}{\rho_s I_s + \rho_f I_f}}. \tag{1}$$

Here, ρ_f is the fluid density, ρ_s is the waveguide density, μ is its shear modulus, J is the torsion constant (depending on the geometry of the waveguide), I_s is the polar inertia of the waveguide and I_f is the apparent inertia of the fluid.

2. METHOD

2.1. THE DIFFERENT STEPS

Use will be made of Hamilton's principle, which states that [7] "among all the displacements that satisfy the presented boundary conditions and the prescribed conditions at $t = t_1$ and $t = t_2$, the actual solution renders the integral $\int_{t_1}^{t_2} (\tilde{T} - \tilde{V} + \tilde{W})\,\mathrm{d}t$ stationary, i.e.,

$$\delta \int_{t_1}^{t_2} (\tilde{T} - \tilde{V} + \tilde{W})\,\mathrm{d}t = 0. \tag{2}$$

In this integral, $\tilde{T}$ denotes the kinetic energy of the system, $\tilde{V}$ denotes the potential energy, and $\tilde{W}$ is the work done by the external forces acting on the system".

It seems easier to first solve the problem for a harmonic excitation, and then go back to the transient problem by an inverse Fourier transform. Write $\tilde{f}$ for a time-dependent function, and, in the harmonic regime, $\tilde{f} = \Re(f\mathrm{e}^{-\mathrm{i}\omega t})$. Equation (2) is then written as

$$\delta(T - V + W) = 0. \tag{3}$$

The mechanical system is the waveguide. External forces acting on it are due to both the torsion momentum imposed at one end of the waveguide and the fluid pressure on the bar boundary. The corresponding works are respectively W_1 and W_2, with $W = W_1 + W_2$.

The variational method requires the following steps:

- approximation of T and V in terms of θ, the torsion angle, based on the asumption that the transverse dimension of the guide is "small" (section 3);
- solving the exterior Neumann problem for the Helmholtz equation in the compressible fluid, to get the expression of the pressure exerted by the fluid (a long-wavelength approximation will be used), from which $W_2(\theta)$ derives (section 4);
- applying equation (3), to get an approximated torsion equation and the phase velocity of the torsional wave (section 5).

Then, application to water-level measurement can be considered (section 6).

2.2. ELLIPTIC CO-ORDINATES AND MATHIEU FUNCTIONS

On the grounds mentioned below, the cross-section of the waveguide is supposed to be elliptic. Thus, the Neumann problem for the Helmholtz equation has an analytical solution, using elliptic co-ordinates (which leads to solutions in terms of Mathieu functions). Moreover, experiments [4] showed that with such a geometry, the torsional wave is quite sensitive to the external fluid characteristics.

2.2.1. *Some properties of elliptic co-ordinates* (*see reference* [8] *for example*)

Referring to Figure 3, any point M can be described by its elliptic co-ordinates (ξ, η), related to its Cartesian co-ordinates (x_1, x_2) by

$$\begin{aligned} x_1 &= h \cosh \xi \cos \eta, \\ x_2 &= h \sinh \xi \sin \eta, \end{aligned} \tag{4}$$

where h is the half-interfocal distance of any ellipse $\xi = \text{constant}$ (and any hyperbola $\eta = \text{constant}$).

Later on, the following relations between elliptic (A_ξ, A_η) and Cartesian (A_1, A_2) co-ordinates of a vector $\mathbf{A}$ will be needed:

$$\begin{aligned} A_\xi &= \frac{\cos \eta \sinh \xi \; A_1 + \sin \eta \cosh \xi \; A_2}{\sqrt{\cosh^2 \xi - \cos^2 \eta}}, \\ A_\eta &= \frac{-\sin \eta \cosh \xi \; A_1 + \cos \eta \sinh \xi \; A_2}{\sqrt{\cosh^2 \xi - \cos^2 \eta}}. \end{aligned} \tag{5}$$

For the elliptic cylinder, a third co-ordinate z, with $z = x_3$ is used.

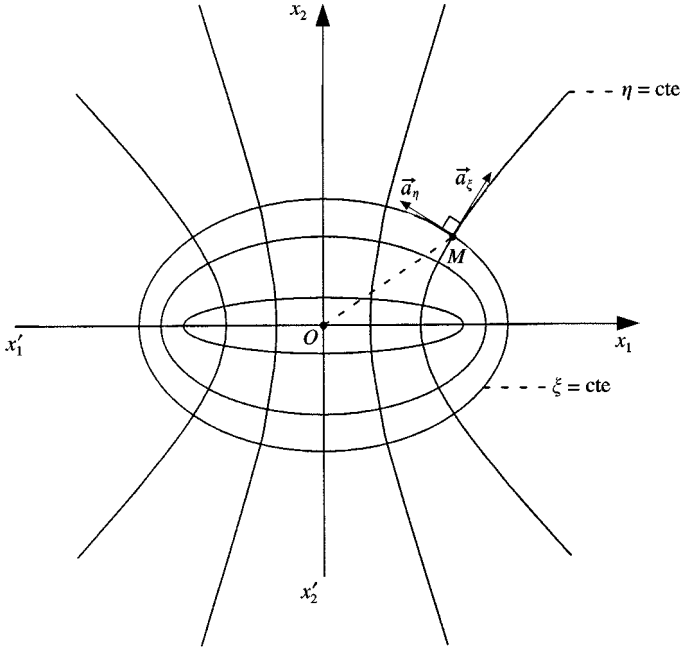

Figure 3. System of elliptic co-ordinates.

2.2.2. *Mathieu functions* (*see references* [9, 10]).

Consider the Helmholtz equation in elliptic co-ordinates:

$$\frac{1}{h^2(\cosh^2\xi - \cos^2\eta)}\left(\frac{\partial^2\phi}{\partial\xi^2} + \frac{\partial^2\phi}{\partial\eta^2}\right) + k^2\phi = 0. \tag{6}$$

Looking for a solution with separated variables, $\phi(\xi,\eta) = \phi_\xi(\xi)\,\phi_\eta(\eta)$, one gets

$$\frac{\phi''_\xi}{\phi_\xi} + k^2h^2\cosh^2\xi = k^2h^2\cos^2\eta - \frac{\phi''_\eta}{\phi_\eta} \tag{7}$$

from which

$$\phi''_\eta + (\gamma - k^2h^2\cos^2\eta)\,\phi_\eta = 0 \tag{8}$$

and

$$\phi''_\xi - (\gamma - k^2h^2\cosh^2\xi)\,\phi_\xi = 0 \tag{9}$$

where γ is the separation constant.

For the function $\phi_\eta(\eta)$ to be periodic, the separation constant γ can take a countable sequence of values only. The subsequences corresponding to even and odd functions are denoted by γ^e_m and γ^o_m respectively. Thus, the periodic general solution of equation (8) takes the form

$$\begin{aligned}
\phi_\eta(\eta) &= \sum_{m=0}^{\infty} a^e_m\,\mathrm{S}^e_m(kh,\cos\eta), \quad \gamma = \gamma^e_m, \quad m = 0,1,2,\ldots,\\
\phi_\eta(\eta) &= \sum_{m=1}^{\infty} a^o_m\,\mathrm{S}^o_m(kh,\cos\eta), \quad \gamma = \gamma^o_m, \quad m = 1,2,3,\ldots.
\end{aligned} \tag{10}$$

$\mathrm{S}^e_m(kh,\cos\eta)$ and $\mathrm{S}^o_m(kh,\cos\eta)$ are respectively the even and odd Mathieu functions of the first kind and order m.

Later on, only the odd Mathieu functions of the first kind are involved. Use will be made of

- their expansion into Fourier series:

$$\begin{aligned}
\mathrm{S}^o_{2m}(kh,\cos\eta) &= \sum_{n=1}^{\infty} B^o_{2n}(kh,2m)\sin(2n\eta),\\
\mathrm{S}^o_{2m+1}(kh,\cos\eta) &= \sum_{n=0}^{\infty} B^o_{2n+1}(kh,2m+1)\sin((2n+1)\eta);
\end{aligned} \tag{11}$$

- the definition of their norm:

$$\int_0^{2\pi} \mathrm{S}^o_m(kh,\cos\eta)\mathrm{S}^o_n(kh,\cos\eta)\,\mathrm{d}\eta = \delta^n_m M^o_m(kh). \tag{12}$$

Then, the general solution of equation (9) corresponding to the same separation constants takes the form

$$\phi_\xi(\xi) = \sum_{m=0}^{\infty} \{c_m^e \, \mathrm{J}_m^e(kh, \cosh\xi) + d_m^e \, \mathrm{N}_m^e(kh, \cosh\xi)\}, \quad \gamma = \gamma_m^e, \; m = 0, 1, \ldots,$$
$$\phi_\xi(\xi) = \sum_{m=1}^{\infty} \{c_m^o \, \mathrm{J}_m^o(kh, \cosh\xi) + d_m^o \, \mathrm{N}_m^o(kh, \cosh\xi)\}, \quad \gamma = \gamma_m^o, \; m = 1, 2, \ldots. \tag{13}$$

$\mathrm{J}_m^e(kh, \cosh\xi)$ and $\mathrm{J}_m^o(kh, \cosh\xi)$ are the modified Mathieu functions of first kind and order m; $\mathrm{N}_m^e(kh, \cosh\xi)$ and $\mathrm{N}_m^o(kh, \cosh\xi)$ are the modified Mathieu functions of second kind and order m.

The following notations are also used:

$$H_m^e = \mathrm{J}_m^e + \mathrm{i}\,\mathrm{N}_m^e,$$
$$H_m^o = \mathrm{J}_m^o + \mathrm{i}\,\mathrm{N}_m^o. \tag{14}$$

3. TORSION OF THE WAVEGUIDE *IN VACUO*

It is assumed that:

- the torsion results in a small deformation of the waveguide, so that the torsion of a cross-section is approximated by a rotation;
- the wavelengths in the waveguide are much larger than the dimensions of its cross-section. As a consequence, the torsion angle θ is supposed to depend only on z;
- the length L of the waveguide is much larger than any characteristic dimension of its cross-section. As a result, the exterior forces acting on the waveguide boundary σ are small compared to the interior forces due to the torsion. Thus, a stress-free boundary condition on σ will be written.

Let $\mathscr{M}(\beta)$ be a torsion momentum imposed at the end $z = \beta$ of the waveguide. Then

$$\delta W_1 = \mathscr{M}(\beta)\,\delta\theta(\beta). \tag{15}$$

To establish the expressions of T and V, classical methods of continuum mechanics are used. Landau and Lifchitz [11] will be followed.

3.1. RELATION BETWEEN THE TRANSVERSE COMPONENTS OF THE DISPLACEMENT AND THE TORSION ANGLE

Consider any point $P(x_1, x_2)$ in the cross-section, before deformation. After deformation, the cross-section has turned and P is at $P'(x_1 + u_1, x_2 + u_2)$ (see Figure 4).

Polar co-ordinates (ρ, φ) are used to get the expressions for u_1 and u_2:

$$P\begin{cases} x_1 = \rho\cos\varphi, \\ x_2 = \rho\sin\varphi, \end{cases} \quad P'\begin{cases} x_1 + u_1 = \rho\cos(\varphi + \theta), \\ x_2 + u_2 = \rho\sin(\varphi + \theta). \end{cases} \tag{16}$$

Then

$$u_1 = x_1(\cos\theta - 1) - x_2\sin\theta,$$
$$u_2 = x_2(\cos\theta - 1) + x_1\sin\theta. \tag{17}$$

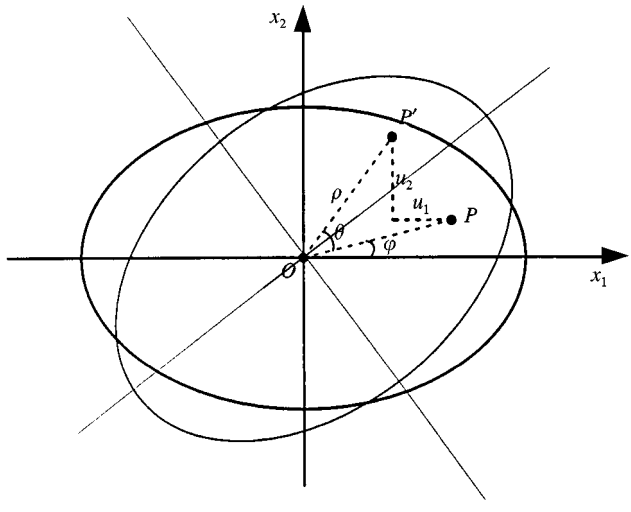

Figure 4. Torsion of a cross-section.

As the angle θ is small, one can replace $\cos\theta$ and $\sin\theta$ by the first term of their Taylor series:

$$\cos\theta = 1 + \mathcal{O}(\theta^2),$$
$$\sin\theta = \theta + \mathcal{O}(\theta^3). \tag{18}$$

One finally gets

$$u_1 = -x_2\,\theta + \mathcal{O}(\theta^2),$$
$$u_2 = x_1\,\theta + \mathcal{O}(\theta^3). \tag{19}$$

Applying equation (5), one gets the expression of the transverse components of the displacement in elliptic co-ordinates:

$$u_\xi = \frac{h\cos\eta\sin\eta}{\sqrt{\cosh^2\xi - \cos^2\eta}}\,\theta,$$
$$u_\eta = \frac{h\cosh\xi\sinh\xi}{\sqrt{\cosh^2\xi - \cos^2\eta}}\,\theta. \tag{20}$$

To get the expression of u_z, more considerations are needed. They are dealt with in the next sections.

3.2. CONSEQUENCE OF THE STRESS-FREE BOUNDARY CONDITION

First look for the expression of the stress components in the bar.

Staying within the frame of linear elasticity, any component U_{ij} of the strain tensor $\boldsymbol{U}$ can be written in terms of the components u_i of the displacement $\mathbf{u}$:

$$U_{ij} = \tfrac{1}{2}(u_{i,j} + u_{j,i}), \tag{21}$$

where $u_{i,j} = \partial u_i / \partial x_j$. Inserting equation (19) in equation (21), one gets

$$\boldsymbol{U} = \begin{pmatrix} 0 & 0 & \frac{1}{2}(-x_2\theta_{,3} + u_{3,1}) \\ 0 & 0 & \frac{1}{2}(x_1\theta_{,3} + u_{3,2}) \\ \frac{1}{2}(-x_2\theta_{,3} + u_{3,1}) & \frac{1}{2}(-x_1\theta_{,3} + u_{3,2}) & u_{3,3} \end{pmatrix}, \tag{22}$$

λ and μ being the Lamé coefficients of the bar. Hooke's law is written as

$$\sigma_{ij} = \lambda \mathrm{Tr}\boldsymbol{U}\delta_i^j + 2\mu U_{ij} \tag{23}$$

which leads to

$$\boldsymbol{\sigma} = \begin{pmatrix} \lambda u_{3,3} & 0 & \mu(-x_2\theta_{,3} + u_{3,1}) \\ 0 & \lambda u_{3,3} & \mu(x_1\theta_{,3} + u_{3,2}) \\ \mu(-x_2\theta_{,3} + u_{3,1}) & \mu(x_1\theta_{,3} + u_{3,2}) & (\lambda + 2\mu)u_{3,3} \end{pmatrix}. \tag{24}$$

As mentioned at the beginning of section 3, one can neglect the exterior forces which act on the waveguide boundary. This stress-free boundary condition is written on σ as

$$\sigma_{ij} n_j = 0, \tag{25}$$

where $\mathbf{n}$ is the unit vector normal to σ and pointing out to the waveguide exterior. One can infer from (24) that, on this surface:

$$u_{3,3} = 0,$$

$$(-x_2\theta_{,3} + u_{3,1})n_1 + (x_1\theta_{,3} + u_{3,2})n_2 = 0. \tag{26}$$

The first equality (26) gives

$$u_3 = C\,\phi(x_1, x_2) \tag{27}$$

where C is a constant. Using the second equation (26), one gets, on σ:

$$(x_2 n_1 - x_1 n_2)\theta_{,3} = C(\phi_{,1} n_1 + \phi_{,2} n_2). \tag{28}$$

As a result, $\theta_{,3}$ is constant on σ. Without loss of generality, one can choose

$$\theta_{,3} = C \tag{29}$$

Finally, on the boundary σ:

$$u_3 = \phi(x_1, x_2)\theta_{,3} \tag{30}$$

where ϕ, which is called the *torsion function*, is the solution of

$$\phi_{,1} n_1 + \phi_{,2} n_2 = x_2 n_1 - x_1 n_2. \tag{31}$$

Equation (30) implies that, in the interior of the bar, u_3 has the following form:

$$u_3(x_1, x_2, x_3) = \phi(x_1, x_2)\theta_{,3} + v_3(x_1, x_2, x_3) \tag{32}$$

with

$$v_3(x_1, x_2, x_3) = 0 \quad \text{on } \sigma. \tag{33}$$

According to the assumption that the transverse dimensions of the waveguide are small, v_3 can be expanded into a Taylor series as

$$v_3(x_1, x_2, x_3) = v_3(0, 0, x_3) + x_1 v_{3,1}(0, 0, x_3) + x_2 v_{3,2}(0, 0, x_3) + \cdots . \tag{34}$$

The condition (33) gives

$$v_3(0, 0, x_3) = 0. \tag{35}$$

Thus, as a first order approximation,

$$v_3(x_1, x_2, x_3) = 0. \tag{36}$$

As a result, u_3 has the form (30) everywhere.

3.3. THE TORSION FUNCTION AND THE LONGITUDINAL COMPONENT OF THE DISPLACEMENT

From equation (31), one has, on the bar boundary σ:

$$(-x_2 + \phi_{,1})n_1 + (x_1 + \phi_{,2})n_2 = 0 \tag{37}$$

which is a first condition on ϕ.

Moreover, the equilibrium of the bar is written as

$$\sigma_{ij,j} = 0 \tag{38}$$

which, from equations (24), (29) and (30), gives the second condition on ϕ:

$$\Delta\phi = 0; \tag{39}$$

ϕ can then be determined. For an elliptic cross-section with half-axes a and b, the torsion function is [12, section 36]

$$\phi = -\frac{(a^2 - b^2)}{(a^2 + b^2)} x_1 x_2. \tag{40}$$

The three components of the displacement can now be written. The first approximation is

$$\begin{aligned} u_1 &= -x_2\theta, \\ u_2 &= x_1\theta, \\ u_3 &= \phi(x_1, x_2)\theta_{,3}. \end{aligned} \tag{41}$$

3.4. KINETIC ENERGY OF THE WAVEGUIDE

From equation (41), one gets

$$u_{1,t} = -x_2\tilde{\theta}_{,t},$$
$$u_{2,t} = x_1\tilde{\theta}_{,t}, \tag{42}$$
$$u_{3,t} = \phi(x_1, x_2)\tilde{\theta}_{,3t}.$$

By definition

$$\tilde{T} = \int_{x_3}\int\int_{\mathscr{E}}\left[\frac{1}{2}\rho_s(u_{1,t}^2 + u_{2,t}^2 + u_{3,t}^2)\right]\mathrm{d}\mathscr{E}\,\mathrm{d}x_3, \tag{43}$$

so

$$\tilde{T} = \int_{x_3}\frac{1}{2}\rho_s I_s\tilde{\theta}_{,t}^2\,\mathrm{d}x_3 + \int_{x_3}\frac{1}{2}\rho_s P\tilde{\theta}_{,3t}^2\,\mathrm{d}x_3 \tag{44}$$

with

$$I_s = \int\int_{\mathscr{E}}(x_1^2 + x_2^2)\,\mathrm{d}\mathscr{E}; \quad P = \int\int_{\mathscr{E}}\phi^2(x_1, x_2)\,\mathrm{d}\mathscr{E}. \tag{45}$$

I_s is the polar inertia of the waveguide, and P is its warping inertia. For an elliptic cross-section,

$$I_s = \frac{\pi ab}{4}(a^2 + b^2); \quad P = \frac{\pi a^3b^3(a^2 - b^2)^2}{24(a^2 + b^2)^2}. \tag{46}$$

Finally, from equation (44) one gets the following expression of T in the harmonic regime:

$$T = \int_{x_3}\frac{1}{2}\rho_s I_s\omega^2\theta\theta^*\,\mathrm{d}x_3 + \int_{x_3}\frac{1}{2}\rho_s P\omega^2\theta_{,3}\theta_{,3}^*\,\mathrm{d}x_3. \tag{47}$$

Now, in the present case, θ is a real function.

3.5. POTENTIAL ENERGY OF THE WAVEGUIDE

V is written in terms of the strain and stress tensors as

$$V = \int_{x_3}\int\int_{\mathscr{E}}\frac{1}{2}\sigma_{ij}U_{ij}\,\mathrm{d}\mathscr{E}\,\mathrm{d}x_3. \tag{48}$$

From equations (41), (22) and (24), one gets

$$V = \int_{x_3}\frac{1}{2}\mu J\theta_{,3}^2\,\mathrm{d}x_3 \tag{49}$$

with

$$J = \iint_{\mathscr{E}} (x_1^2 + x_2^2 + x_1\phi_{,2} - x_2\phi_{,1})\,\mathrm{d}\mathscr{E} \tag{50}$$

the torsion constant. For an elliptic cross-section, we have

$$J = \frac{\pi a^3 b^3}{(a^2 + b^2)}. \tag{51}$$

4. THE EXTERIOR NEUMANN PROBLEM IN THE FLUID

4.1. THE TERMS OF THE PROBLEM

Because a compressible fluid is being considered, acoustic radiation into the fluid has to be accounted for.

First, consider the problem of an infinite fluid. Then, because the aim is to measure fluid levels, a partially immersed waveguide will be considered. The fluid occupies a half-space only, with a free surface on which the acoustic pressure is zero.

4.1.1. *In an infinite fluid*

To solve the problem easily, the cylinder is supposed to be baffled (Figure 5).

Let $\sigma(\xi = \xi_0, \alpha \leqslant z \leqslant \beta)$ be the waveguide boundary, and Ω its exterior, which contains the fluid. At a point of σ, call $\mathbf{n}$ the unit vector normal to σ and pointing out to the waveguide interior. Considering a harmonic $\mathrm{e}^{-\mathrm{i}\omega t}$ motion, the acoustic pressure $p(M)$ at a point $M(\xi, \eta, z)$ in the fluid satisfies the following boundary value problem:

$$\begin{aligned} &(\Delta + k_f^2)\,p(M) = 0 && \text{in} \quad \Omega, \\ &\partial_n p(M) = \rho_f\,\omega^2 u_n && \text{for} \quad \xi = \xi_0, \alpha \leqslant z \leqslant \beta, \\ &\qquad = 0 && \text{for} \quad \xi = \xi_0, z < \alpha \bigcup z > \beta, \\ &\text{Limit absorption principle,} \end{aligned} \tag{52}$$

where ω is the angular frequency, k_f is the wave number in the fluid, and u_n is the normal component of the waveguide displacement.

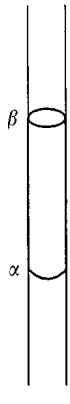

Figure 5. The baffled waveguide.

Let $\delta_{M'}(M)$ be the Dirac measure at $M'(\xi', \eta', z')$. The Green function of the problem will satisfy

$$\begin{aligned} &(\Delta_{(\xi,\eta,z)} + k_f^2)\,\mathcal{G}(M, M') = \delta_{M'}(M) \quad \text{in } \Omega, \\ &\partial_n \mathcal{G} = 0 \qquad\qquad\qquad\qquad\quad \text{for } \xi = \xi_0, \\ &\text{Limit absorption principle,} \end{aligned} \tag{53}$$

where $\Delta_{(\xi,\eta,z)}$ denotes the Laplacian for which the terms with derivatives with respect to the three co-ordinates ξ, η and z are taken into account.

Now taking the space Fourier transform of equation (53), defined by

$$\hat{f}(Z) = \langle f(z),\, \mathrm{e}^{-2\mathrm{i}\pi z Z} \rangle \tag{54}$$

One has:

$$\Delta_{(\xi,\eta)} \hat{\mathcal{G}}(\xi, \xi', \eta, \eta', Z, z') + K_f^2 \hat{\mathcal{G}}(\xi, \xi', \eta, \eta', Z, z') = \mathrm{e}^{-2\mathrm{i}\pi Z z'} \delta_{\xi'}(\xi) \otimes \delta_{\eta'}(\eta) \tag{55}$$

with $K_f^2 = k_f^2 - 4\pi^2 Z^2$; $K_f > 0$ if $K_f^2 > 0$, and $\Im K_f > 0$ otherwise.

So

$$\hat{\mathcal{G}}(\xi, \xi', \eta, \eta', Z, z') = \mathrm{e}^{-2\mathrm{i}\pi z Z}\, G_{K_f}(\xi, \xi', \eta, \eta'), \tag{56}$$

where $G_{K_f}(\xi, \xi', \eta, \eta')$ is defined by

$$\begin{cases} \Delta_{(\xi,\eta)} G_{K_f}(\xi, \xi', \eta, \eta') + K_f^2 G_{K_f}(\xi, \xi', \eta, \eta') = \delta_{\xi'}(\xi) \otimes \delta_{\eta'}(\eta) & \text{in } \Omega, \\ \partial_n G_{K_f} = 0 & \text{for } \xi = \xi_0, \\ \text{Limit absorption principle.} \end{cases} \tag{57}$$

Then, $G_{K_f} = G^I_{K_f} + G^D_{K_f}$, where $G^I_{K_f}$ is the free field Green function; and $G^D_{K_f}$ is the diffracted field. It satisfies the homogeneous Helmholtz equation, a non-homogeneous boundary condition, and the limit absorption principle.

The Green representation of the space Fourier transform of the pressure in the fluid is written as

$$\hat{p}(\xi, \eta, Z) = -\langle \hat{\mathcal{G}}(\xi, \xi_0, \eta, \eta', Z, z')\,{}_{\eta', z'},\, \partial_n p(\xi_0, \eta', z')\, \delta_\sigma(\xi_0, \eta', z') \rangle, \tag{58}$$

where $\langle .\,{}_{\eta', z'}, . \rangle$ means that the integration variables of the duality product are η' and z'.

Then, to get $p(\xi_0, \eta, z)$, the inverse space Fourier transform of $\hat{p}(\xi, \eta, Z)$ must be evaluated. To obtain an analytical result, a long-wavelength approximation is used.

The elementary work done by the fluid pressure on the waveguide can then be calculated:

$$\delta W_2 = \iint_\sigma p\, \mathbf{n} \,.\, \delta \mathbf{u}\, \mathrm{d}\sigma. \tag{59}$$

4.1.2. *Taking into account the surface of the fluid*

Until now, the waveguide was considered to be immersed in an infinite fluid. However, there is the interface between the fluid and the air, on which the pressure should be zero. The

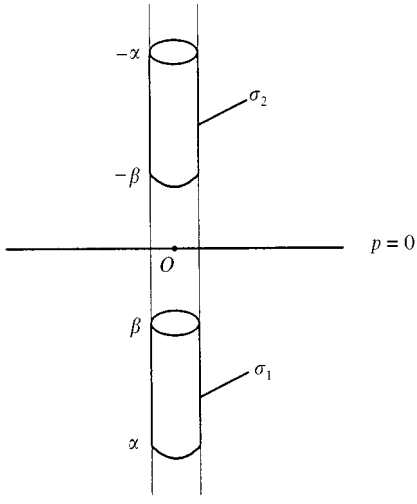

Figure 6. The method of images.

method of images, illustrated in Figure 6, will be used: the free surface is at $z = 0$. The waveguide, with $\alpha \leqslant z \leqslant \beta$, has a side boundary named σ_1. Its image, with $-\beta \leqslant z \leqslant -\alpha$, has a side boundary named σ_2.

The new problem is written in the same way as the previous one, but with $\sigma = \sigma_1 + \sigma_2$. The Green function is the same, but the boundary conditions for the pressure are expressed differently:

$$\begin{aligned} \partial_n p(M) &= \rho_f \omega^2 u_n(\eta, z) \qquad \text{on } \sigma_1, \\ \partial_n p(M) &= -\rho_f \omega^2 u_n(\eta, -z) \quad \text{on } \sigma_2. \end{aligned} \tag{60}$$

Then, equation (58) is changed into

$$\begin{aligned} \hat{p}(\xi, \eta, Z) = &- \langle \hat{\mathscr{G}}(\xi, \xi_0, \eta, \eta', Z, z')_{\eta', z'} \, \partial_n p(\xi_0, \eta', z') \, \delta_{\sigma_1}(\xi_0, \eta', z') \rangle \\ &- \langle \hat{\mathscr{G}}(\xi, \xi_0, \eta, \eta', Z, z')_{\eta', z'} \, \partial_n p(\xi_0, \eta', z') \, \delta_{\sigma_2}(\xi_0, \eta', z') \rangle. \end{aligned} \tag{61}$$

The problem is treated in section 4.5. Initially the focus is on an infinite fluid.

4.2. THE SPACE FOURIER TRANSFORM OF THE GREEN FUNCTION

In this section, we look for the expression of

$$\hat{\mathscr{G}}(\xi, \xi', \eta, \eta', Z, z') = \mathrm{e}^{-2\mathrm{i}\pi z Z} (G^I_{K_f}(\xi, \xi', \eta, \eta') + G^D_{K_f}(\xi, \xi', \eta, \eta')). \tag{62}$$

From reference [13, p. 1421],

$$\begin{aligned} G^I_{K_f}(M, M') = &- \mathrm{i} \left\{ \sum_{m=0}^{\infty} \frac{\mathrm{S}^e_m(K_f h, \cos \eta')}{M^e_m(K_f h)} \mathrm{S}^e_m(K_f h, \cos \eta) \mathrm{J}^e_m(K_f h, \cosh \xi) H^e_m(K_f h, \cosh \xi') \right. \\ &\left. + \sum_{m=1}^{\infty} \frac{\mathrm{S}^o_m(K_f h, \cos \eta')}{M^o_m(K_f h)} \mathrm{S}^o_m(K_f h, \cos \eta) \mathrm{J}^o_m(K_f h, \cosh \xi) H^o_m(K_f h, \cosh \xi') \right\} \end{aligned} \tag{63}$$

for $\xi < \xi'$

$$= -\mathrm{i}\left\{\sum_{m=0}^{\infty}\frac{\mathrm{S}_m^e(K_f h,\cos\eta')}{M_m^e(K_f h)}\mathrm{S}_m^e(K_f h,\cos\eta)\,\mathrm{J}_m^e(K_f h,\cosh\xi')H_m^e(K_f h,\cosh\xi)\right.$$

$$\left.+\sum_{m=1}^{\infty}\frac{\mathrm{S}_m^o(K_f h,\cos\eta')}{M_m^o(K_f h)}\mathrm{S}_m^o(K_f h,\cos\eta)\,\mathrm{J}_m^o(K_f h,\cosh\xi')H_m^o(K_f h,\cosh\xi)\right\}$$

for $\xi' < \xi$.

Because $G_{K_f}^D$ has to verify the homogeneous Helmholtz equation and the limit absorption principle, an expression of the following form is sought:

$$G_{K_f}^D(M,M') = \sum_{m=0}^{\infty} a_m^o(K_f h,\cosh\xi',\cos\eta')\,\mathrm{S}_m^o(K_f h,\cos\eta)H_m^o(K_f h,\cosh\xi) \tag{64}$$

$$+\sum_{m=0}^{\infty} a_m^e(K_f h,\cosh\xi',\cos\eta')\mathrm{S}_m^e(K_f h,\cos\eta)H_m^e(K_f h,\cosh\xi)$$

and a_m^o and a_m^e are calculated so that the condition $\partial_\xi G_{K_f}(M,M') = 0$ for $\xi = \xi_0$ is verified. One finds that

$$a_m^e(K_f h,\cosh\xi',\cos\eta') = \mathrm{i}\frac{\mathrm{S}_m^e(K_f h,\cos\eta')}{M_m^e(K_f h)}\mathrm{J}_m^{e\prime}(K_f h,\cosh\xi_0)\frac{H_m^e(K_f h,\cosh\xi')}{H_m^{e\prime}(K_f h,\cosh\xi_0)} \quad \forall m$$

$$a_m^o(K_f h,\cosh\xi',\cos\eta') = \mathrm{i}\frac{\mathrm{S}_m^o(K_f h,\cos\eta')}{M_m^o(K_f h)}\mathrm{J}_m^{o\prime}(K_f h,\cosh\xi_0)\frac{H_m^o(K_f h,\cosh\xi')}{H_m^{o\prime}(K_f h,\cosh\xi_0)} \quad \forall m \geqslant 1 \tag{65}$$

$$a_0^o(K_f h,\cosh\xi',\cos\eta') = 0.$$

Finally,

$$\hat{\mathscr{G}}(\xi,\xi',\eta,\eta',Z,z') \tag{66}$$

$$= \mathrm{e}^{-2\mathrm{i}\pi Z z'}\,G_{K_f}(\xi,\xi',\eta,\eta')$$

$$= \mathrm{i}\,\mathrm{e}^{-2\mathrm{i}\pi Z z'}\left\{\sum_{m=0}^{\infty}\frac{\mathrm{S}_m^e(K_f h,\cos\eta')}{M_m^e(K_f h)}\mathrm{S}_m^e(K_f h,\cos\eta)H_m^e(K_f h,\cosh\xi')\right.$$

$$\times\left(\frac{H_m^e(K_f h,\cosh\xi)\,\mathrm{J}_m^{e\prime}(K_f h,\cosh\xi_0) - \mathrm{J}_m^e(K_f h,\cosh\xi)H_m^{e\prime}(K_f h,\cosh\xi_0)}{H_m^{e\prime}(K_f h,\cosh\xi_0)}\right)$$

$$+\sum_{m=1}^{\infty}\frac{\mathrm{S}_m^o(K_f h,\cos\eta')}{M_m^o(K_f h)}\mathrm{S}_m^o(K_f h,\cos\eta)H_m^o(K_f h,\cosh\xi')$$

$$\left.\left(\frac{H_m^o(K_f h,\cosh\xi)\,\mathrm{J}_m^{o\prime}(K_f h,\cosh\xi_0) - \mathrm{J}_m^o(K_f h,\cosh\xi)H_m^{o\prime}(K_f h,\cosh\xi_0)}{H_m^{o\prime}(K_f h,\cosh\xi_0)}\right)\right\}$$

for $\xi < \xi'$

$$= \mathrm{i}\,\mathrm{e}^{-2\mathrm{i}\pi Z z'}\left\{\sum_{m=0}^{\infty}\frac{\mathrm{S}_m^e(K_f h,\cos\eta')}{M_m^e(K_f h)}\mathrm{S}_m^e(K_f h,\cos\eta)H_m^e(K_f h,\cosh\xi)\right.$$

$$\times\left(\frac{H_m^e(K_f h,\cosh\xi')\,\mathrm{J}_m^{e\prime}(K_f h,\cosh\xi_0)-\mathrm{J}_m^e(K_f h,\cosh\xi')H_m^{e\prime}(K_f h,\cosh\xi_0)}{H_m^{e\prime}(K_f h,\cosh\xi_0)}\right)$$

$$+\sum_{m=1}^{\infty}\frac{\mathrm{S}_m^o(K_f h,\cos\eta')}{M_m^o(K_f h)}\mathrm{S}_m^o(K_f h,\cos\eta)H_m^o(K_f h,\cosh\xi)$$

$$\left.\times\left(\frac{H_m^o(K_f h,\cosh\xi')\,\mathrm{J}_m^{o\prime}(K_f h,\cosh\xi_0)-\mathrm{J}_m^o(K_f h,\cosh\xi')H_m^{o\prime}(K_f h,\cosh\xi_0)}{H_m^{o\prime}(K_f h,\cosh\xi_0)}\right)\right\}$$

for $\xi' < \xi$

4.3. THE SPACE FOURIER TRANSFORM OF THE PRESSURE

4.3.1. *In the fluid*

The Green representation of the space Fourier transform of the pressure in the fluid is written as

$$\hat{p}(\xi,\eta,Z) = -\langle\hat{\mathscr{G}}(\xi,\xi_0,\eta,\eta',Z,z')_{\eta',z'}\partial_n p(\xi_0,\eta',z')\,\delta_\sigma(\xi_0,\eta',z')\rangle. \tag{67}$$

From equation (52), for $z'\in\sigma$,

$$\partial_n p(\xi_0,\eta',z') = \rho_f\,\omega^2 u_n(\xi_0,\eta',z') \tag{68}$$

with, from equation (20);

$$u_n(\xi_0,\eta',z') = -u_{\xi_0}(\xi_0,\eta',z') = -\frac{h\cos\eta'\sin\eta'}{\sqrt{\cosh^2\xi_0-\cos^2\eta'}}\theta(z'). \tag{69}$$

Moreover, in elliptic co-ordinates;

$$\mathrm{d}\sigma(\xi_0,\eta',z') = h\sqrt{\cosh^2\xi_0-\cos^2\eta'}\,\mathrm{d}\eta'\,\mathrm{d}z'. \tag{70}$$

Now write

$$\theta_{[\alpha,\beta]}(z) = \begin{cases}\theta(z) & \text{if } \alpha\leqslant z\leqslant\beta,\\ 0 & \text{otherwise.}\end{cases} \tag{71}$$

Then

$$\begin{aligned}\hat{p}(\xi,\eta,Z) &= \langle\mathrm{e}^{-2\mathrm{i}\pi Z z'}\,G_{K_f}(\xi,\xi_0,\eta,\eta')_{\eta',z'}\rho_f\omega^2h^2\cos\eta'\sin\eta'\,\theta_{[\alpha,\beta]}(z')\rangle\\ &= \rho_f\omega^2h^2\hat{\theta}_{[\alpha,\beta]}(Z)\langle G_{K_f}(\xi,\xi_0,\eta,\eta')_{\eta'}\cos\eta'\sin\eta'\rangle\end{aligned} \tag{72}$$

$\eta' \to \cos\eta' \sin\eta'$ is an odd function in η'. Thus, one does not need the even terms in G_{K_f}. So write that

$$\hat{p}(\xi, \eta, Z) = \rho_f \omega^2 h^2 \hat{\theta}_{[\alpha,\beta]}(Z) \langle G^o_{K_f}(\xi, \xi_0, \eta, \eta')_{,\eta'} \cos\eta' \sin\eta' \rangle. \tag{73}$$

From (67),

$$\begin{aligned} G^o_{K_f}(\xi, \xi_0, \eta, \eta') &= \mathrm{i} \sum_{m=1}^{\infty} \frac{\mathrm{S}^o_m(K_f h, \cos\eta')}{M^o_m(K_f h)} \mathrm{S}^o_m(K_f h, \cos\eta) H^o_m(K_f h, \cosh\xi) \\ &\quad \times \left(\frac{H^o_m(K_f h, \cosh\xi_0)\, \mathrm{J}^o_m{}'(K_f h, \cosh\xi_0) - \mathrm{J}^o_m(K_f h, \cosh\xi_0) H^o_m{}'(K_f h, \cosh\xi_0)}{H^o_m{}'(K_f h, \cosh\xi_0)} \right) \end{aligned} \tag{74}$$

The last numerator of equation (74) is a Wronskian which equals $(-\mathrm{i})$ for the considered functions. So one gets

$$\begin{aligned} \hat{p}(\xi, \eta, Z) &= \rho_f \omega^2 h^2 \hat{\theta}_{[\alpha,\beta]}(Z) \\ &\quad \times \sum_{m=1}^{\infty} \left(\frac{\mathrm{S}^o_m(K_f h, \cos\eta)}{M^o_m(K_f h)} \frac{H^o_m(K_f h, \cosh\xi)}{H^o_m{}'(K_f h, \cosh\xi_0)} \langle \mathrm{S}^o_m(K_f h, \cos\eta')_{,\eta'} \cos\eta' \sin\eta' \rangle \right) \\ &= \rho_f \omega^2 \frac{\pi h^2}{2} \hat{\theta}_{[\alpha,\beta]}(Z) \\ &\quad \times \sum_{m=1}^{\infty} \frac{\mathrm{S}^o_{2m}(K_f h, \cos\eta)}{M^o_{2m}(K_f h)} \frac{H^o_{2m}(K_f h, \cosh\xi)}{H^{o\prime}_{2m}(K_f h, \cosh\xi_0)} B^o_2(K_f h, 2m) \end{aligned} \tag{75}$$

4.3.2. *On the waveguide boundary*

Writing $\xi = \xi_0$ in equation (75), one finally has

$$\begin{aligned} \hat{p}(\xi_0, \eta, Z) &= \rho_f \omega^2 \frac{\pi h^2}{2} \hat{\theta}_{[\alpha,\beta]}(Z) \\ &\quad \times \sum_{m=1}^{\infty} \frac{\mathrm{S}^o_{2m}(K_f h, \cos\eta)}{M^o_{2m}(K_f h)} \frac{H^o_{2m}(K_f h, \cosh\xi_0)}{H^o_{2m}{}'(K_f h, \cosh\xi_0)} B^o_2(K_f h, 2m). \end{aligned} \tag{76}$$

4.4. LONG-WAVELENGTH APPROXIMATION

4.4.1. *The space Fourier transform of the pressure*

With such an expression of $\hat{p}(\xi_0, \eta, Z)$, one cannot get an analytical expression of the inverse space Fourier transform. Noting that in the frequency range of the torsional wave (around 100 kHz), the wavelength λ in the fluid is much larger than the characteristic dimension of the cross-section, a "long-wavelength approximation" will be sought.

Therefore, Mathieu functions will be first expressed in terms of Bessel and Neumann functions (see reference [13, pp. 1568–1573]). An approximation in terms of a truncated series of the successive powers of $(K_f h)$ is sought. To this aim, the function $\hat{p}$ is expanded into a formal Taylor series of $(K_f h)$ around $K_f h = 0$.

$$\begin{aligned}\hat{p}(\xi_0, \eta, Z) \simeq & -\rho_f \omega^2 h^2 \hat{\theta}_{[\alpha,\beta]}(Z) \\ & \times \left\{ \left(\frac{1}{4} + \frac{(e^{-2\xi_0} + 3e^{2\xi_0})}{192} (K_f h)^2 \right) \sin(2\eta) - \frac{(K_f h)^2}{192} \sin(4\eta) \right\}\end{aligned} \tag{77}$$

4.4.2. *The inverse space Fourier transform of the pressure approximation*

Take the inverse Fourier transform of each term, assuming that the result will be, at least, an asymptotic series. Now compute the lowest order term. Writing

$$A = h^2 \frac{(e^{-2\xi_0} + 3e^{2\xi_0})}{192} \quad \text{and} \quad B = \frac{h^2}{192} \tag{78}$$

one gets

$$\begin{aligned} & p(\xi_0, \eta, z) \\ & = \langle \hat{p}(\xi_0, \eta, Z) \underset{Z}{,} e^{2i\pi z Z} \rangle \\ & \simeq -\rho_f \omega^2 h^2 \left(\left(\frac{1}{4} + A k_f^2 \right) \sin(2\eta) - B k_f^2 \sin(4\eta) \right) \langle \hat{\theta}_{[\alpha,\beta]}(Z) \underset{Z}{,} e^{2i\pi z Z} \rangle \\ & \quad - \rho_f \omega^2 h^2 (A \sin(2\eta) - B \sin(4\eta)) \langle -4\pi^2 Z^2 \hat{\theta}_{[\alpha,\beta]}(Z) \underset{Z}{,} e^{2i\pi z Z} \rangle \end{aligned} \tag{79}$$

which gives

$$\begin{aligned} p(\xi_0, \eta, z) \simeq & -\rho_f \omega^2 h^2 \left\{ \left(\left(\frac{1}{4} + A k_f^2 \right) \sin(2\eta) - B k_f^2 \sin(4\eta) \right) \theta_{[\alpha,\beta]}(z) \right. \\ & \left. + \left(A \sin(2\eta) - B \sin(4\eta) \right) \frac{\partial^2 \theta_{[\alpha,\beta]}}{\partial z^2} \right\}. \end{aligned} \tag{80}$$

4.4.3. *Calculation of the work done by the fluid pressure*

The work done by the fluid pressure while the bar is submitted to an elementary rotation $\delta\theta$ is written as

$$\begin{aligned} \delta W_2 &= \int\int_\sigma p \mathbf{n} \cdot \delta \mathbf{u}(\delta\theta) \, d\sigma \\ &= -\int_{-\alpha}^{\beta} \int_0^{2\pi} p(\xi_0, \eta, z) \, \delta u_{\xi_0}(\delta\theta) \, h \sqrt{\cosh^2 \xi_0 - \cos^2 \eta} \, d\eta \, dz. \end{aligned} \tag{81}$$

Using equations (80) and (20), one finally gets

$$\delta W_2 \simeq \int_\alpha^\beta \rho_f \omega^2 \frac{\pi h^4}{2} \left\{ \theta(z) \left(\frac{1}{4} + A k_f^2 \right) + A \frac{\partial^2 \theta}{\partial z^2} \right\} \delta\theta \, dz. \tag{82}$$

4.5. TAKING INTO ACCOUNT THE FREE SURFACE OF THE FLUID

From equations (60) with (20),

$$\partial_n p(M) \simeq \begin{cases} -\rho_f h\,\omega^2 \dfrac{\cos\eta \sin\eta}{\sqrt{\cosh^2\xi_0 - \cos^2\eta}}\,\theta(z) & \text{on } \sigma_1, \\ \rho_f h\,\omega^2 \dfrac{\cos\eta \sin\eta}{\sqrt{\cosh^2\xi_0 - \cos^2\eta}}\,\theta(-z) & \text{on } \sigma_2. \end{cases} \tag{83}$$

Then, following the method developed in section 4.3, one gets

$$\hat{p}(\xi, \eta, Z) \simeq \rho_f\,\omega^2 h^2 \langle G^o_{K_f}(\xi, \xi_0, \eta, \eta') \underset{\eta'}{,} \cos\eta' \sin\eta' \rangle (\hat{\theta}_{[\alpha,\beta]}(Z) - \hat{\theta}_{[\alpha,\beta]}(-Z)). \tag{84}$$

So, on the waveguide boundary,

$$\hat{p}(\xi_0, \eta, Z) \simeq \rho_f\,\omega^2 \frac{\pi h^2}{2} (\hat{\theta}_{[\alpha,\beta]}(Z) - \hat{\theta}_{[\alpha,\beta]}(-Z)) \times \sum_{m=1}^{\infty} \frac{S^o_{2m}(K_f h, \cos\eta)}{M^o_{2m}(K_f h)} \frac{H^o_{2m}(K_f h, \cosh\xi_0)}{H^o_{2m}{}'(K_f h, \cosh\xi_0)} B^o_2(K_f h, 2m) \tag{85}$$

and, after the long-wavelength approximation,

$$\hat{p}(\xi_0, \eta, Z) \simeq -\rho_f \omega^2 h^2 (\hat{\theta}_{[\alpha,\beta]}(Z) - \hat{\theta}_{[\alpha,\beta]}(-Z)) \times \left\{ \left(\frac{1}{4} + \frac{(e^{-2\xi_0} + 3e^{2\xi_0})}{192} (K_f h)^2 \right) \sin(2\eta) - \frac{(K_f h)^2}{192} \sin(4\eta) \right\}. \tag{86}$$

The inverse space Fourier transform gives

$$p(\xi_0, \eta, z) \simeq -\rho_f \omega^2 h^2 \times \left\{ \left(\frac{1}{4} + A k_f^2 \sin(2\eta) - B k_f^2 \sin(4\eta) \right) (\theta_{[\alpha,\beta]}(z) - \theta_{[\alpha,\beta]}(-z)) + (A \sin(2\eta) - B \sin(4\eta)) \left(\frac{\partial^2 \theta_{[\alpha,\beta]}(z)}{\partial z^2} - \frac{\partial^2 \theta_{[\alpha,\beta]}(-z)}{\partial z^2} \right) \right\}. \tag{87}$$

Then, calculate

$$\delta W_2 = \int\int_{\sigma} p\mathbf{n} \cdot \delta\mathbf{u}(\delta\theta)\,\mathrm{d}\sigma. \tag{88}$$

In the end, one finds (82) again that

$$\delta W_2 \simeq \int_{\alpha}^{\beta} \rho_f\,\omega^2 \frac{\pi h^4}{2} \left\{ \theta(z) \left(\frac{1}{4} + A k_f^2 \right) + A \frac{\partial^2 \theta}{\partial z^2} \right\} \delta\theta\,\mathrm{d}z. \tag{89}$$

So, due to the approximation of the Mathieu functions for long wavelength, one sees that the free surface has no influence on the previous results.

5. THE APPROXIMATE TORSION EQUATION OF THE FLUID-LOADED BAR

Now all the elements namely, equations (15), (44), (49) and (82), to apply Hamilton's principle (3) to the functions with a harmonic time dependence have been obtained, the integration being taken over an integer number of periods. The following approximate torsion equation is obtained:

$$\left(\mu J + \rho_f \omega^2 A \frac{\pi h^4}{2}\right)\frac{\partial^2 \theta}{\partial z^2} + \left(\rho_s I_s + \rho_f \frac{\pi h^4}{2}\left(\frac{1}{4} + A\frac{\omega^2}{c_f^2}\right)\right)\omega^2 \theta(z) = 0. \tag{90}$$

From equation (90), the following expression of the apparent phase velocity is obtained

$$c(\omega) \simeq \sqrt{\frac{\left(\mu J + \rho_f A \dfrac{\pi h^4}{2}\omega^2\right)}{\left(\rho_s I_s + \rho_f \dfrac{\pi h^4}{2}\left(\dfrac{1}{4} + A\dfrac{\omega^2}{c_f^2}\right)\right)}} \tag{91}$$

which can be compared with that obtained for an incompressible fluid (1). It emphasizes the influence of the fluid, as:

- an additional stiffness, $\rho_f A(\pi h^4/2)\omega^2$, which was neglected by previous authors;
- an additional inertia, $\rho_f(\pi h^4/2)(1/4 + A(\omega^2/c_f^2))$, which has two components: the component given by previous authors, $\rho_f \pi h^4/8$, and an added one, $\rho_f(\pi h^4/2)A\omega^2/c_f^2$, which is due to the compressibility of the fluid.

Figure 7 highlights the importance of these added terms for water at the conditions of a pressurized water reactor. The waveguide is in stainless steel, with $\mu = 7{\cdot}57 \times 10^{10}$ Pa and $\rho_s = 7900$ kg/m^3; the cross-section is elliptic, with $a = 3$ mm and $b = 1$ mm; the water at $1{\cdot}55 \times 10^7$ Pa and 325°C has a density of $\rho_f = 662$ kg/m^3 [14], and $c_f = 783$ m/s (from reference [15]). In these conditions, the simulation given in Figure 7 shows that the correction on the apparent phase velocity brought by the model may reach 4·7% at 150 kHz.

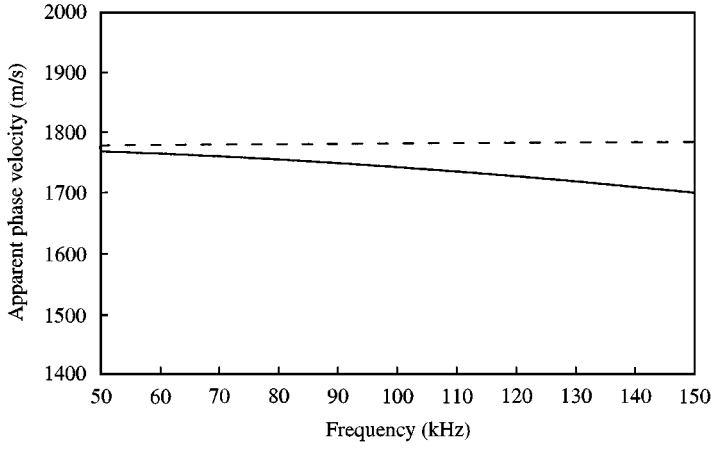

Figure 7. The apparent phase velocity of the torsional wave propagating in a waveguide immersed in water at $1{\cdot}55 \times 10^7$ Pa and 325°C, as a function of the excitation frequency. – – –: incompressible fluid model; ——: compressible fluid model.

6. SIMULATION OF THE FLUID-LEVEL MEASUREMENT

It is assumed that the signal spectrum has a small bandwidth centered around an angular frequency ω_0. Thus, the fluid-loaded waveguide can be considered as a medium with a constant torsional velocity $c(\omega_0)$. Now consider a partially immersed waveguide, as presented in Figure 8. Δt, the total propagation time, is experimentally measured. The unknown parameter is α_L.

The propagation time Δt can be written as $\Delta t = 2(\Delta t_1 + \Delta t_2)$, where Δt_1 is the propagation time in the first part of the bar (of length $L(1 - \alpha_L)$), and Δt_2 the propagation time in the immersed part of the bar (of length $\alpha_L L$). Let c_0 be the *in vacuo* phase velocity, practically in air. Then

$$c_0 = \sqrt{\frac{\mu J}{\rho_s I_s}}. \tag{92}$$

The apparent phase velocity in the immersed part is $c(\omega)$, given by (91).

One can now decompose Δt as

$$\Delta t = 2\left(\frac{L(1 - \alpha_L)}{c_0} + \frac{\alpha_L L}{c(\omega)}\right). \tag{93}$$

α_L is finally deduced from equation (93):

$$\alpha_L = \frac{c(\omega)}{c_0 - c(\omega)}\left(\frac{\Delta t c_0}{2L} - 1\right). \tag{94}$$

To highlight the improvement given by the model, simulations were made, considering surrounding fluids which emphasized the discrepancy between the case for which the compressibility is taken into account and the case for which it is not. Among the different fluids, the one that could be used on a scale model in laboratory, in the near future was chosen. It was decided to work with methylene iodide. Its required characteristics are $\rho_f = 3324$ kg/m^3 and $c_f = 973$ m/s [16]. Consider a frequency of 100 kHz. The waveguide has the same characteristics as in section 5. Its length is supposed to be $L = 3$ m.

Figure 9 shows the propagation time of the torsional wave in terms of α_L. The correction brought by the model reaches 4% for a completely immersed waveguide.

Figure 10 highlights the pertinence of the corrective terms for the application to fluid-level measurement. Indeed, the simulation shows calculated α_L in terms of the

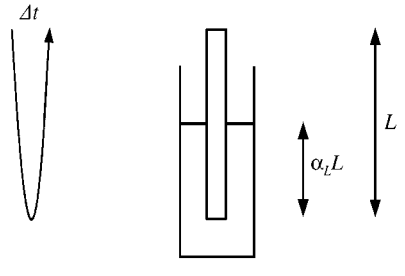

Figure 8. Partially immersed waveguide for fluid-level measurement.

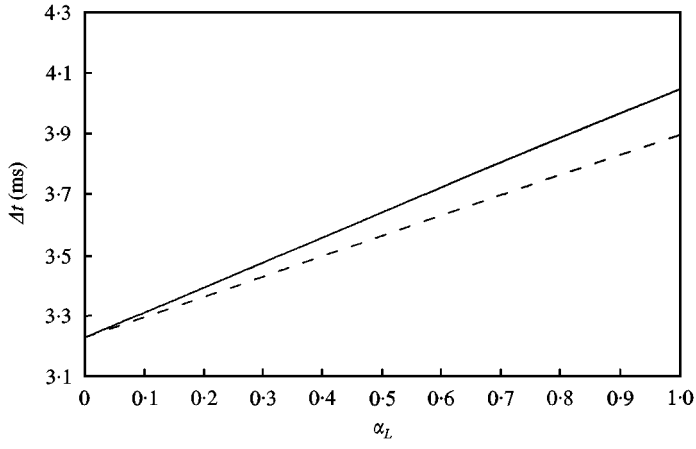

Figure 9. Propagation time of the torsional wave in the waveguide partially immersed in methylene iodide successively considered as compressible and incompressible, as a function of the immersed length. – – –: $(\Delta t)_{inc.}$; ——: $(\Delta t)_{comp.}$.

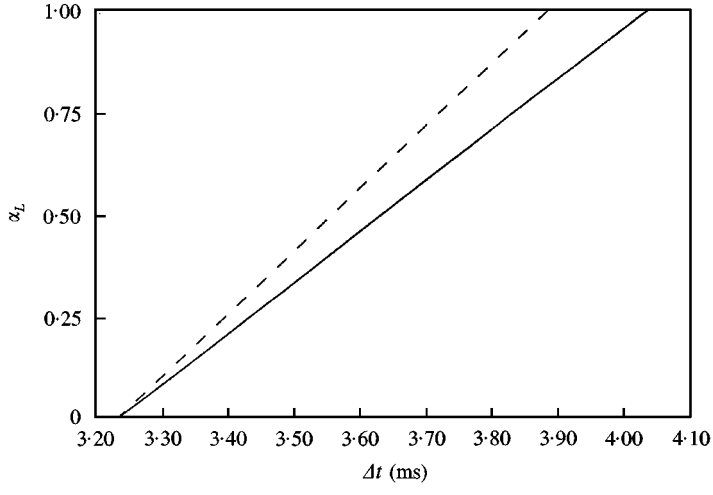

Figure 10. α_L calculated from the propagation time of the torsional wave in the waveguide partially immersed in methylene iodide: – – –, incompressible fluid model; ——, compressible fluid model.

propagation time, comparing the case for which compressibility is taken into account with the case for which it is not. For example, the added terms induce a correction of 18·8 % on α_L for a measured propagation time of 3·85 ms.

As underlined before (see section 1.3), taking the compressibility of the surrounding fluid into account is only a first step in the improvement of the model. Indeed, in a reactor vessel, the fluid can turn into a two-phase fluid. Formula (91) requires expressions of ρ_f and c_f, the equivalent density and sound velocity of the two-phase fluid. This implies having a model which correctly describes the reactor conditions. As a first example, consider a simple model of a two-phase fluid: water with a given density of uniform-sized air bubbles. It is assumed that the radius of the bubbles is smaller than 500 μm, the resonance frequency of the bubbles is much higher than the frequency of the torsional wave (100 kHz), and the

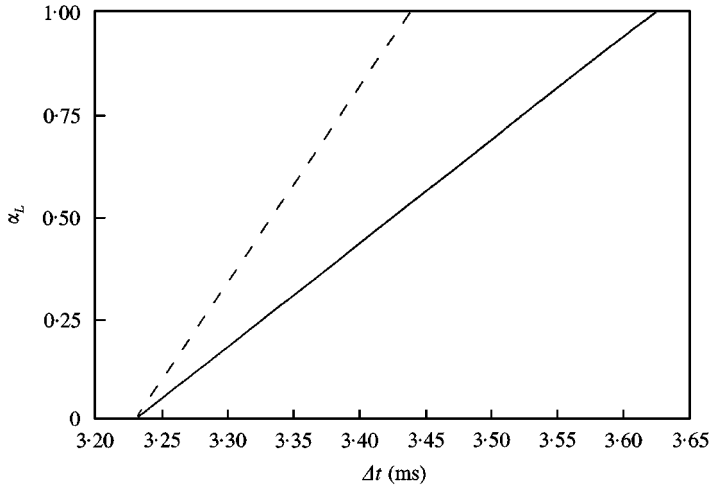

Figure 11. α_L calculated from the propagation time of the torsional wave in the waveguide partially immersed in a mixture of water and uniform-sized air bubbles, with a void fraction of 3×10^{-4}: – – –, incompressible fluid model; ——, compressible fluid model.

wavelengths in the waveguide are larger than the radius of the bubbles. Under those conditions, the density of the mixture and the speed of sound in it are written from reference [17] as

$$\rho_f = \tau\rho_a + (1-\tau)\,\rho_w,$$

$$c_f = \frac{1}{\sqrt{\dfrac{(1-\tau)^2}{c_w^2} + \dfrac{\tau^2}{c_a^2} + \dfrac{\tau(1-\tau)\rho_w}{\gamma P_0}}}, \tag{95}$$

where τ is the void fraction of the mixture (for our simulation, $\tau = 3 \times 10^{-4}$), $\rho_w = 998$ kg/m^3 is the density of water, $\rho_a = 1{\cdot}3$ kg/m^3 is the density of air, $c_w = 1500$ m/s is the speed of sound in water, $c_a = 330$ m/s is the speed of sound in air, $\gamma = 1{\cdot}4$ is the ratio of specific heats and $P_0 = 101\,300$ Pa is the atmospheric pressure.

Figure 11 shows calculated α_L in terms of the propagation time of the torsional wave. It compares the results obtained by considering the mixture as an incompressible fluid with ρ_f from equation (95) with the results from the improved model, with ρ_f and c_f from equation (95). The added terms induce a correction of 47% on α_L for a measured propagation time of 3·43 ms.

7. CONCLUDING REMARKS

This work focused on the propagation of a torsional wave in a waveguide immersed in a compressible fluid. An approximate analytical expression of the apparent phase velocity of the wave has been obtained. It shows the influence of the compressibility of the fluid, and depends on the frequency of the wave, on the geometry of the waveguide, and on the celerity of waves in the fluid considered. Then, this result has been applied to fluid-level measurement. Simulations were made, which showed that the correction brought by our improved model may be significant.

In the near future, some experiments will be carried out. We also plan to improve the theoretical model by considering a two-phase fluid.

REFERENCES

1. A. E. ARAVE 1979 *NRC Instrumentation Review Group Meeting, Silver Spring, Maryland*. Ultrasonic densitometer development.
2. H. H. BAU 1986 *ASME Journal of Applied Mechanics* **53**, 846–848. Torsional wave sensor — a theory.
3. Y. WANG 1987 *Ph.D. Thesis, University of Pennsylvania*. The effects of adjacent viscous fluid on the transmission of torsional stress waves in a solid waveguide.
4. J. O. KIM 1989 *Ph.D. Thesis, University of Pennsylvania*. The interaction between stress waves transmitted in solid waveguides and adjacent media.
5. J. O. KIM, H. H. BAU, Y. LIU, L. C. LYNNWORTH, S. A. LYNNWORTH, K. A. HALL, S. A. JACOBSON, J. A. KORBA, R. J. MURPHY, M. A. STRAUCH and K. G. KING 1993 *IEEE Transactions on Ultrasonics, Ferroelectrics, and Frequency Control* **40**, 563–574. Torsional sensor applications in two-phase fluids.
6. M. A. FRIESEL 1996 *Review of Scientific Instruments* **67**, 1574–1576. Proposed improvements for torsional wave measurements of density and viscosity.
7. F. FAHY 1985 *Sound and Structural Vibration*. Academic Press.
8. N. W. MCLACHLAN 1947 *Theory and Application of Mathieu Functions*. Oxford: Oxford University Press.
9. K. HONG and J. KIM 1995 *Journal of Sound and Vibration* **183**, 327–351. Natural mode analysis of hollow and annular elliptical cylindrical cavities.
10. F. P. MECHEL 1997 *Mathieu Functions*. S. Hirzel-Verlag.
11. L. LANDAU and E. LIFCHITZ 1959 *Course of Theoretical Physics. VII: Theory of Elasticity*. Oxford: Pergamon Press.
12. I. S. SOKOLNIKOFF 1956 *Mathematical Theory of Elasticity*. New-York: McGraw-Hill.
13. P. M. MORSE and H. FESHBACH 1953 *Methods of Theoretical Physics*. New York: McGraw-Hill.
14. E. SCHMIDT 1969 *Properties of Water and Steam in SI Units*. Berlin: Springer-Verlag.
15. L. C. LYNNWORTH 1989 *Ultrasonic Measurements for Process Control. Theory, Techniques, Applications*. New York: Academic Press.
16. I. S. GRIGORIEV and E. Z. MEILIKHOV 1997 *Handbook of Physical Quantities*. Boca Raton, FL: CRC Press.
17. P. ARZELIES 1981 *Ph.D. Thesis, Université d'Aix-Marseille II*. Acoustique des bulles. Contribution à l'étude de la propagation en milieu diphasique liquide-bulles de gaz. Problème inverse, identification de paramètres décrivant le milieu.